CHARACTERIZATION OF SUPPORTED NICKEL CATALYSTS PREPARED BY DEPOSITION OF NICKEL CHLORIDE VAPOR ON ALUMINA

YOSHIMITSU UEMURA, YASUO HATATE AND ATSUSHI IKARI
Department of Chemical Engineering, Kagoshima University, Kagoshima 890

Key Words: Material, Nickel Alumina Catalyst, Nickel Particle Size, Nickel Concentration Profile, Electron Probe Microanalysis, Transmission Electron Microscopy, Vapor Deposition Method, Acetylene Hydrogenation

Nickel/alumina catalysts were prepared by the deposition of nickel chloride vapor on spherical alumina (3.5 mm diameter) followed by reduction. This paper describes the effects of preparation conditions (deposition time and deposition temperature) on the nickel content, the nickel concentration profile, and the nickel particle diameter.

The nickel content increased with increasing deposition time of nickel chloride vapor, and decreased with increasing deposition temperature. The average nickel particle diameters were observed by TEM, and were not affected substantially by deposition time or deposition temperature. They ranged from 500 to 650 nm. The intraparticle penetration of nickel proceeded with increasing deposition time. The activation energy of acetylene hydrogenation was about 50 kJ·mol^{-1}, regardless of the preparation method, which involves gas phase method and impregnation method. The activity per unit surface area of nickel showed the following order: vapor deposition nickel/alumina > gas phase reduction nickel ≃ impregnated nickel/alumina.

Introduction

Liquid-phase methods, such as impregnation or precipitation, are commonly used industrially for preparing supported metal catalysts. These methods involve many processes such as impregnation, washing, drying, calcination, and activation in the impregnation method. Such complication is mainly due to the use of solvents. The most common solvent is water, which has undesirable effects on supports and active material precursors on the support. As chemical effects, dissolving[14] and hydration[1] of the support were reported. As a physical effect, redistribution of the active material precursor in the support during drying was reported.[7,9] To prevent such undesirable effects, investigations of a solvent[13] or a solution[10] were carried out. Recently, some workers developed a gas-phase method as a preparation technique, in which vapor of an active material precursor was used: 1) titania fine particles[8,12] and nickel fine particles[11] prepared by chemical vapor deposition (in other words, by gas-phase reaction), 2) nickel/silica prepared by chemical vapor decomposition,[15] 3) platinum/alumina prepared by vacuum deposition,[2] and 4) supported molybdenum oxide prepared by adsorption of a molybdenum compound vapor.[6] Such a method may eliminate the problems of the impregnation method. To establish the gas-phase method, however, further investigations are needed.

In previous studies, we investigated the effects of support nature,[17-19] nickel content,[16,18,20] solvent of impregnant,[18] post-impregnation drying condition,[16,17,19] and nickel source material[20] on the physical properties and reactivity of nickel/alumina impregnated catalysts. In this work, the characterization of nickel/alumina catalysts prepared by the deposition of nickel chloride vapor on alumina (a gas-phase method) was undertaken to investigate the effects of deposition condition on the characteristics of the catalysts.

1. Experimental

1.1 Preparation

1) Equipment Nickel/alumina catalysts were prepared by the vapor-deposition method using the apparatus shown in **Figs. 1** and **2**. High-surface area spherical alumina of 3.5 mm diameter (JRC-ALO-1 supplied by Catalysis Society of Japan, **Table 1**) was used as a support and anhydrous nickel chloride (guaranteed grade of Kanto Chemical Co. Ltd.) was used as a nickel source material.

The reactor (10) was a mullite tube of 35 mm internal diameter and 1000 mm length. A support holder (8) and a nickel chloride holder (9) were provided in the upper part of the reactor (14, deposition zone) and in the lower part (15, vaporization zone), respectively. The temperatures of the deposition zone (14) and the vaporization zone (15) were

Received March 7, 1988. Correspondence concerning this article should be addressed to Y. Uemura.

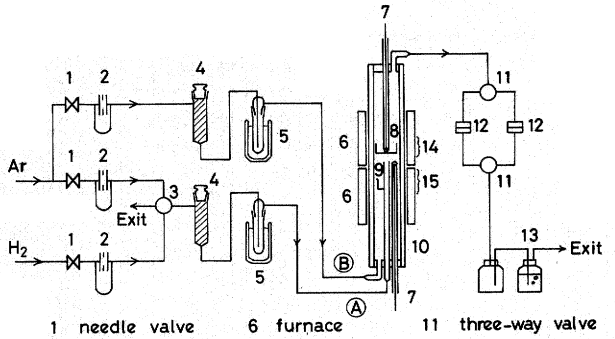

Fig. 1. Schematic diagram of experimental apparatus

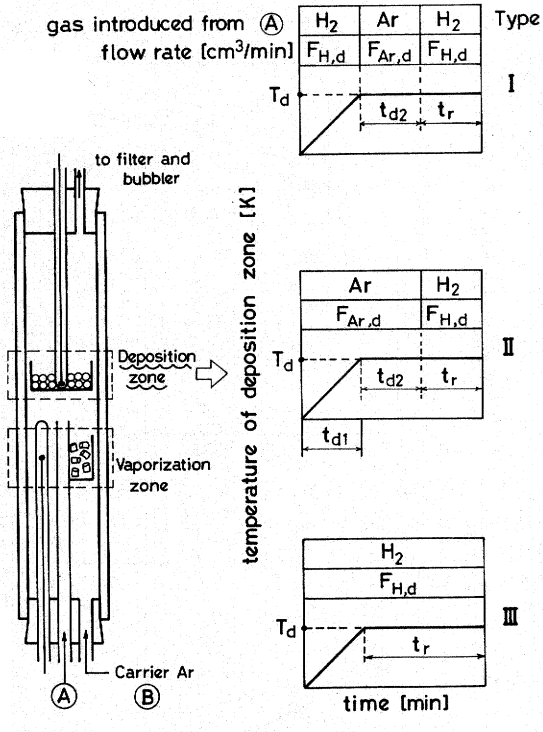

Fig. 2. Procedure of deposition

Table 1. Physical properties of JRC-ALO-1

Form	White sphere
Composition	$\eta+\gamma$-alumina[5]
BET surface area [$m^2 \cdot kg^{-1}$]	1.69×10^5 [4]
Modal pore diameter [nm]	9.0[5]
Specific pore volume [$m^3 \cdot kg^{-1}$]	6.70×10^{-4} [5]

maintained at desired values by electric furnaces (6). The temperature in each zone was monitored by a thermocouple (7). Carrier argon was introduced from the entrance Ⓑ. Argon or hydrogen was introduced from the entrance Ⓐ. To prevent the sintering of ALO-1, all the gases were dried by passing them through silica gel columns (4) and dry ice-methanol traps (5). In all experiments, the average partial pressure of nickel chloride vapor in the deposition zone (14) was 0.72 ± 0.08 kPa as estimated from the material balance of nickel chloride.

2) Procedure Three types of operating procedure were applied as illustrated in Fig. 2. The conditions are listed in **Table 2**. As an example, the procedure of type I is described below. About 3 g of pelletized nickel chloride was charged into the holder (9). About 3 g of ALO-1 was charged into the holder (8). The carrier argon at 500 $cm^3 \cdot min^{-1}$ and hydrogen at 100 $cm^3 \cdot min^{-1}$ were introduced from Ⓑ and Ⓐ respectively. The temperature elevation (4.2 ± 0.3 deg $\cdot min^{-1}$) of each zone was started. After attaining desired temperatures, hydrogen from Ⓐ was exchanged for argon by a four-way valve (3). The vaporization zone (15) was maintained at 1073 K. The deposition zone (14) was maintained at a temperature shown in Table 2. After a time period t_{d2}, argon from Ⓐ was replaced by hydrogen, which flowed through during the time period t_r. After cooling to room temperature, samples were separately taken from the reactor—from the upper portion of the holder (upper sample) and from its lower portion (lower sample).

In the present experiments, unsupported nickel fine particles by gas-phase reduction, i.e., the reduction of nickel chloride vapor in bulk gas phase, were also obtained by filtration (12) of the flue gas from the reactor (10).

1.2 Characterization

1) Nickel content The nickel content of each catalyst was determined by titrating the nickel(II) ion in the sample solution prepared by dissolving the nickel of the catalyst in hydrochloric acid and filtering. The nickel content was also measured by an electron probe microanalyser (EPMA, Shimadzu ARL microprobe X-ray analyser) for some catalysts using a point-counting technique.

2) Intraparticle nickel concentration profile Intraparticle nickel concentration profiles were measured by EPMA. The procedure was the same as that described in the previous paper.[20]

3) Morphology of nickel particles Transmission electron microscopy (TEM, Hitachi H-700H) was used to determine the nickel particle diameters and their distribution in the catalyst. The procedure for measurement was the same as that described in the previous paper.[20]

The nickel particles of the catalysts observed by TEM were not spherical. Each diameter, D_p, was calculated from Eq. (1) as the sphere equivalent diameter based on outer surface area. The nickel particle was assumed to be an ellipsoidal body of revolution. Surface mean diameter ($\bar{D}_{p32}$) was calculated from Eq. (2).

$$D_p = \frac{10^6}{f_m f_e}\left[\frac{1}{2}\left\{a^2 + \frac{ab^2}{(b^2-a^2)^{1/2}}\cos^{-1}\left(\frac{a}{b}\right)\right\}\right]^{1/2} \quad (1)$$

Table 2. Preparation conditions

Run No.	Deposition zone							Ni content [wt%]			
	Type (shown in Fig. 2)	T_d [K]	$F_{Ar,d}$ [cm^3·min^{-1}]	$F_{H,d}$ [cm^3·min^{-1}]	t_{d1} [min]	t_{d2} [min]	t_r	Upper sample (HCl method)	Lower sample (HCl method)	Lower sample*1 (EPMA)	Lower sample*2 (EPMA)
G2	III	1073	—	100	—	—	160	(0.17)*3	(0.17)*3	—	—
G3	I	1073	100	100	—	90	90	1.43	1.73	1.1	0.5
G5	I	1033	100	100	—	90	90	1.73	1.86	1.0	0.6
G6	I	1013	100	100	—	90	90	1.96	2.20	1.4	0.9
G7	I	1073	100	100	—	30	90	1.38	1.43	1.0	0.3
G11	II	1073	50	50	195	60	60	2.49	3.15	—	—
G12	II	1073	50	50	196	0	60	1.70	2.42	—	—
G13	II	1073	50	50	201	20	60	1.89	2.77	—	—

*1 300 μm from outer surface.
*2 Center of particle.
*3 The product was not fractionated.

$$\bar{D}_{p32}=\frac{\Sigma D_{pi}^3}{\Sigma D_{pi}^2} \quad (2)$$

About 100 to 200 nickel particles were measured for diameter inspection using at least ten enlarged photographs of 36,000X.

4) Hydrogenation of acetylene The reaction was carried out in an atmospheric flow reactor to compare the catalytic properties of the catalysts. The reactor was made from Pyrex tube of 10 mm internal diameter. Three kinds of catalysts were used: vapor deposition Ni/ALO-1 (G12L), gas-phase reduction Ni (G2FP: nickel fine particles by the reduction of nickel chloride vapor in bulk gas phase in G2), and impregnated Ni/ALO-1 (nickel content 1.4 wt%). The impregnation method was described in the previous study.[16] G2FP was mixed with fine powder of ALO-1, and was pelletized, producing 3.0 wt% G2FP/ALO-1. In the reaction experiments, a sieved fraction from 20 to 100 mesh was used for each catalyst.

About 40 mg of the catalyst was packed into the reactor and pretreated in a stream of hydrogen at 673 K for 1 h. The reaction rate was measured at 370–450 K. The partial pressure of acetylene was 5.1 kPa and that of hydrogen was 40.5 kPa. The total feed rate was 200 cm^3 (NTP)·min^{-1}.

2. Results and Discussion

2.1 Nickel content

The nickel content of each catalyst is shown in Table 2. Deposition of nickel chloride vapor on the alumina support does not occur substantially in the presence of hydrogen (G2). On the other hand, nickel supported on alumina was obtained in G3-G13. As shown in Table 2, the nickel content of each lower sample is larger than that of the upper sample obtained in the same run. This results from the smaller vapor pressure of nickel chloride in the upper section of the alumina bed than that in the lower section. The above description is supported by the material balance of nickel chloride. That is, 8 to 20% of the nickel chloride vapor was adsorbed by the alumina during passing through the bed.

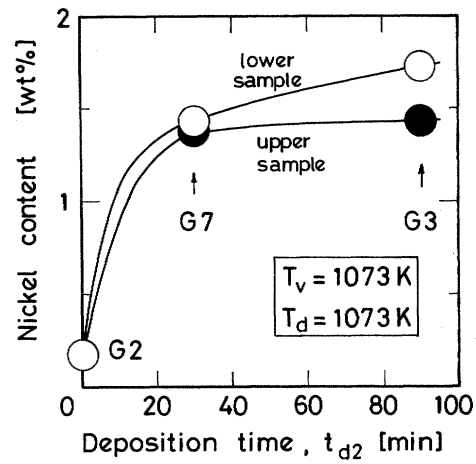

Fig. 3. Effect of deposition time on nickel content

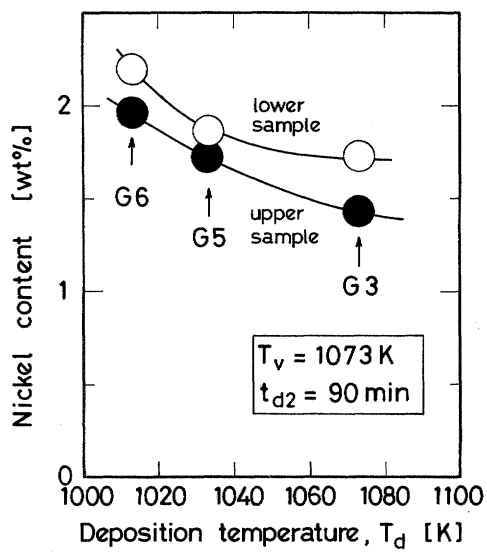

Fig. 4. Effect of deposition temperature on nickel content

In **Figs. 3** and **4**, the effects of deposition time and

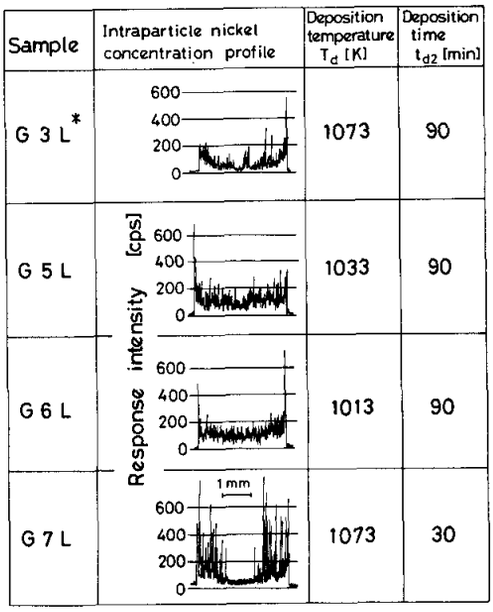

Fig. 5. Nickel concentration profiles (Type I experiments). *"L" refers to the lower sample

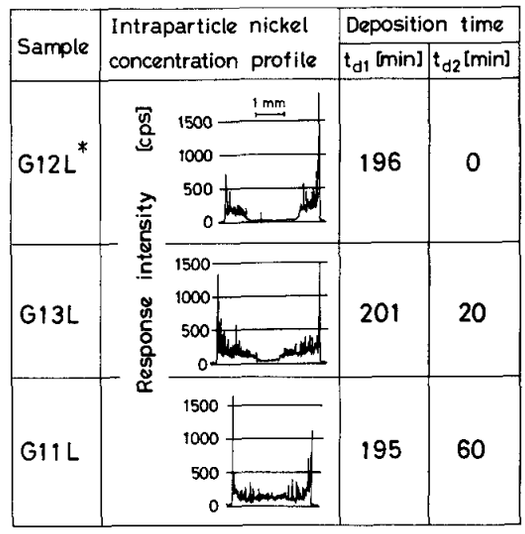

Fig. 6. Nickel concentration profiles (Type II experiments). *"L" refers to the lower sample.

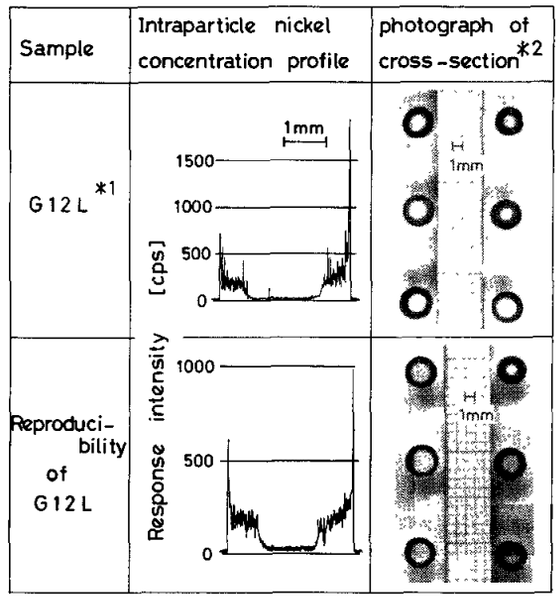

Fig. 7. Result of reproducibility experiment. *1 "L" refers to the lower sample. *2 Six particles in each sample show particle-to-particle reproducibility.

deposition temperature respectively on nickel content are shown. The nickel content increases with increasing deposition time and decreases with increasing deposition temperature.

2.2 Intraparticle nickel concentration profile

The nickel concentration profiles are illustrated in **Figs. 5, 6** and **7**. In Figs. 5 (G3L fand G7L) and 6, the penetration of nickel proceeds with deposition time (t_{d2}). Figure 7 shows the good reproducibility obtained in the present study.

An attempt was made to apply the unreacted core model[21] to those results. In the present case, the incorporation of nickel chloride is analogous to "reaction" in the model. In the case of external mass transfer controlling, the time for complete incorporation is expressed as follows.

$$t^* = \frac{\rho_{ads} R}{3 C_{NiCl_2,b} k_c} \tag{3}$$

In the case of intraparticle diffusion controlling, the time is as follows.

$$t^* = \frac{\rho_{ads} R^2}{6 C_{NiCl_2,b} D_{e,NiCl_2}} \tag{4}$$

The calculated t^* from Eqs. (3) and (4) were about 3 min and 3 h, respectively. The parameters used are presented in **Table 3**. Since it took about 1 h for the complete penetration of nickel layer (Figs. 5 and 6), intraparticle diffusion is supposed to control the intraparticle nickel profile.

Table 3. Model parameters for unreacted core model based on Run G11

ρ_{ads}	[mol·m^{-3}]	5.3×10^2
R	[m]	1.55×10^{-3}
$C_{NiCl_2,b}$	[mol·m^{-3}]	8.1×10^{-2}
k_c	[m·s^{-1}]	1.8×10^{-2} *1
$D_{e,NiCl_2}$	[m^2·s^{-1}]	2.5×10^{-7} *2

*1 Calculated from Yoshida's correlation.[22]
*2 Calculated from Knudsen diffusion coefficient on the assumption that (porosity/tortuosity) = 0.1.

2.3 Morphology of nickel particles

Transmission electron micrographs of G6L, G2FP (nickel fine particles by gas-phase reduction in G2), ALO-1, and impregnated nickel/alumina (nickel content 4.3 wt%)[18] are shown in **Fig. 8**. **Figure 9** shows transmission electron micrographs of G12L under lower magnification. The black images are nickel

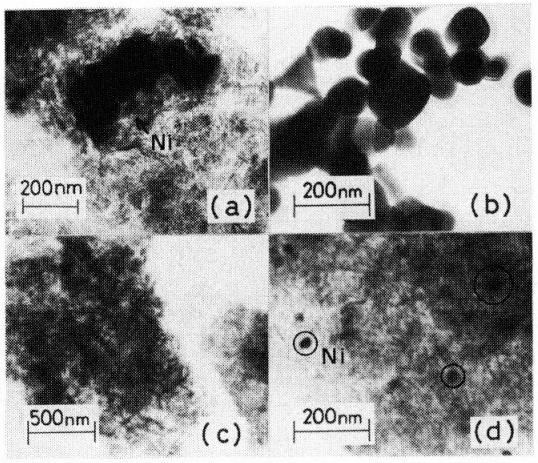

Fig. 8. Transmission electron micrographs: (a), G6L; (b), G2FP (nickel fine particle by the reduction of nickel chloride vapor in bulk gas phase in G2); (c), ALO-1; (d), impregnated nickel/alumina.[18] Black images represent nickel particles.

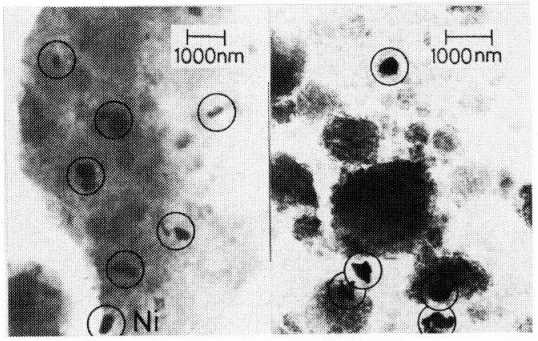

Fig. 9. Transmission electron micrographs of G12L under lower magnification

particles. The nickel particle surface of the typical vapor deposition nickel/alumina (G6L) consists of convex parts and concave parts, whereas that of the gas-phase reduction nickel fine particle (G2FP) is smooth. Neither particle is spherical in most cases. The nickel particle of the impregnated nickel/alumina is smaller than that of gas-phase method nickel/alumina, and is substantially spherical.

The nickel particle size distributions of G2FP and G3L from TEM photographs are illustrated in **Fig. 10**. The particle size distributions and the average sizes of other catalysts (G5L-G7L and G11L-G13L) were similar to those of G3L. It can be seen from the result that the deposition temperature and the deposition time have no significant effect on the distribution and its average diameter (500–650 nm).

It is necessary to discuss whether nickel particles of about 500 nm diameter can be present in the interior of ALO-1, which has 9 nm modal pore diameter. We suppose that this is possible from three kinds of measurements (EPMA, TEM, and mercury porosimetry) for the following reasons. First, the nickel content by EPMA agree with those by the HCl

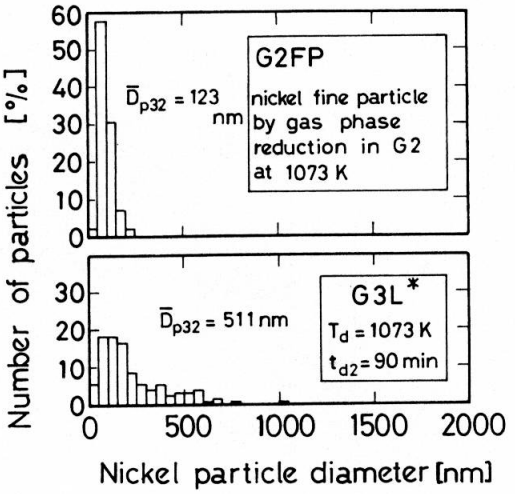

Fig. 10. Nickel particle size distributions. *"L" refers to the lower sample.

dissolving method in consideration of the accuracy of EPMA (Table 2). Second, an outer portion and an inner portion of the catalyst particle (G6L) were individually inspected by TEM. In both inspections, nickel particles of about 500 nm diameter were observed with similar frequency. Third, the partial pore volume of ALO-1 above 500 nm pore diameter was measured three times by a mercury porosimeter. The average partial pore volume was $0.0092\,cm^3 \cdot g^{-1}$ and its standard deviation was $0.0028\,cm^3 \cdot g^{-1}$. The nickel content of 3 wt% is converted to $0.0033\,cm^3$-metal nickel$\cdot$(g-cat.)$^{-1}$, which is less than the partial pore volume ($0.0092\,cm^3 \cdot g^{-1}$). From those results, it appears that nickel particles of about 500 nm diameter can be present in the interior of ALO-1.

The average nickel diameter of G2FP, which is obtained by gas-phase reduction in G2, is 123 nm, about one-fith that of the nickel/alumina prepared by the vapor-deposition method (500–650 nm).

2.4 Hydrogenation of acetylene

The Arrhenius plots of the reaction are presented in **Fig. 11** for three kinds of catalysts, prepared by the three methods described in 1.2. The activation energies are about $50\,kJ \cdot mol^{-1}$ regardless of preparation method, and agree with the values in the literature.[3] The reaction rate per unit surface area of nickel shows the following order: G12L > G2FP/ALO-1 $\simeq$ impregnated Ni/ALO-1. From the results of the morphological study (Section 2.3) and of the reaction study, the nickel particle (about 500 nm diameter) in the vapor-deposition catalysts is thought to be an agglomerated body of smaller nickel particles.

Conclusions

Eight kinds of nickel/alumina catalyst were prepared by the deposition of nickel chloride vapor on an alumina support followed by hydrogen reduction.

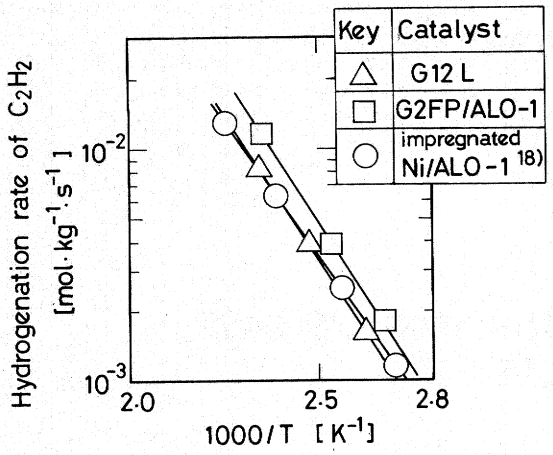

Fig. 11. Arrhenius plots of acetylene hydrogenation

Characterization of the catalysts led to the following conclusions.

1) The support, ALO-1, incorporated nickel chloride vapor at 1013 to 1073 K, whereas nickel(II) ion was not adsorbed by the support in aqueous solution.

2) The nickel content increased with increasing deposition time, and decreased with increasing deposition temperature.

3) The intraparticle penetration of nickel in alumina proceeded with increasing deposition time. Significant nonuniformity disappeared after about 1 h. This phenomenon is interpreted as nickel chloride incorporation under intraparticle diffusion controlling by the application of the unreacted core model.

4) The surface of the nickel particle consisted of convex parts and concave parts. The average diameters were 500 to 650 nm, which were not affected by the deposition time or the deposition temperature.

5) The activation energies of acetylene hydrogenation were about 50 kJ·mol^{-1}, regardless of preparation method, whether gas-phase method or impregnation method. The reaction rate per unit surface area of nickel showed the following order: vapor-deposition nickel/alumina > gas-phase reduction nickel ≃ impregnated nickel/alumina.

Acknowledgement

The authors gratefully acknowledge financial support from a Grant-in-Aid for Scientific Research of the Ministry of Education, Science and Culture, Japan (No. 61750893, 1986).

We also wish to thank Professor S. Morooka of Kyushu University and Associate Professor K. Ikemizu of Tohwa University for their valuable advice.

Nomenclature

a	=	breadth of nickel particle in transmission electron micrograph	[mm]
b	=	length of nickel particle in transmission electron micrograph	[mm]
$C_{NiCl_2,b}$	=	concentration of nickel chloride vapor in bulk fluid	[mol·m^{-3}]
$D_{e,NiCl_2}$	=	effective diffusion coefficient of nickel chloride vapor	[m^2·s^{-1}]
D_p	=	sphere equivalent diameter of nickel particle based on external surface area	[nm]
$\bar{D}_{p32}$	=	surface mean diameter of nickel particle	[nm]
$F_{Ar,d}$	=	gas flow rate of argon introduced from entrance Ⓐ in Fig. 2.	[cm^3·min^{-1}]
$F_{H,d}$	=	gas flow rate of hydrogen introduced from entrance Ⓐ in Fig. 2.	[cm^3·min^{-1}]
f_e	=	enlargement factor from negative to print of transmission electron micrograph	[—]
f_m	=	magnification factor of transmission electron microscope	[—]
k_c	=	mass transfer coefficient	[m·s^{-1}]
R	=	catalyst radius	[m]
T_d	=	temperature in deposition zone	[K]
T_v	=	temperature in vaporization zone	[K]
t_{d1}	=	deposition time during temperature elevation	[min]
t_{d2}	=	deposition time at T_v	[min]
t_r	=	reduction time	[min]
t^*	=	time for complete incorporation of nickel chloride on alumina	[s]
ρ_{ads}	=	saturated incorporation density of nickel chloride on alumina	[mol·m^{-3}]

Literature Cited

1) Archibald, R. C. and R. S. Greensfelder: *Ind. Eng. Chem.*, **37**, 356 (1945).
2) Baker, R. T. K., C. Thomas and R. B. Thomas: *J. Catal.*, **38**, 510 (1975).
3) Bond, G. C.: "Catalysis by Metals," p. 285, Academic Press (1962).
4) Data-JRC-0001, Hattori, T.: *Shokubai* (*Catalyst*), **22**, 115 (1980).
5) Data-JRC-0002, Mukaida, K.: *Shokubai* (*Catalyst*), **22**, 116 (1980).
6) Fransen, T., P. C. van Berge and P. Mars: Proceedings of the First International Symposium on Scientific Bases for the Preparation of Heterogeneous Catalysts, 405 (1976).
7) Galiasso, R., O. L. de Ochoa and P. Andreu: *Appl. Catal.*, **5**, 309 (1983).
8) Kirkbir, F. and H. Komiyama: *Can. J. Chem. Eng.*, **65**, 759 (1987).
9) Komiyama, M., R. P. Merrill and H. F. Harnsberger: *J. Catal.*, **63**, 35 (1980).
10) Kotter, M. and L. Riekert: Preprints for the Second International Symposium on Scientific Bases for the Preparation of Heterogeneous Catalysts, A4 (1978).
11) Morooka, S., A. Kobata, T. Yasutake, K. Ikemizu and Y. Kato: *Kagaku Kogaku Ronbunshu*, **13**, 481 (1987).
12) Morooka, S., T. Yasutake, A. Kobata, K. Ikemizu and Y. Kato: *Kagaku Kogaku Ronbunshu*, **13**, 159 (1987).
13) Murrell, L. L. and D. J. C. Yates: Preprints for the Second International Symposium on Scientific Bases for the Preparation of Heterogeneous Catalysts, C7 (1978).
14) Ozaki, A.: "Shokubai Chosei Kagaku," p. 54, Kodansha (1980).
15) Tsugo, Y., H. Ooi, M. Yano and Y. Harano: Proceedings of World Congress III of Chemical Engineering, Vol. 4, 310 (1986).
16) Uemura, Y., Y. Hatate and A. Ikari: *J. Japan Petrol. Inst.*, **29**, 143 (1986).
17) Uemura, Y., Y. Hatate and A. Ikari: *J. Chem. Eng. Japan*, **19**, 560 (1986).

18) Uemura, Y., Y. Hatate and A. Ikari: *J. Japan Petrol. Inst.*, **30**, 53 (1987).
19) Uemura, Y., Y. Hatate and A. Ikari: *J. Chem. Eng. Japan*, **20**, 117 (1987).
20) Uemura, Y., Y. Hatate and A. Ikari: *J. Chem. Eng. Japan*, **20**, 563 (1987).
21) Yagi, S. and D. Kunii: *Kogyo Kagaku Zasshi*, **56**, 131 (1953).
22) Yoshida, F., D. Ramaswami and O. A. Hougen: *AIChE J.*, **8**, 5 (1962).